Talanta 82 (2010) 1156–1163

Contents lists available at ScienceDirect

Talanta

journal homepage: www.elsevier.com/locate/talanta

Mathematical modeling of a Nafion membrane based optode incorporating 1-(2′-pyridylazo)-2-naphthol under flow injection conditions

Spas D. Kolev[a,*], Terence J. Cardwell[b], Robert W. Cattrall[a,b], Lilibeth dlC. Coo[c]

[a] School of Chemistry, The University of Melbourne, Victoria 3010, Australia
[b] Department of Chemistry, La Trobe University, Victoria 3086, Australia
[c] Institute of Chemistry, University of the Philippines, Diliman, Quezon City 1101, Philippines

ARTICLE INFO

Article history:
Received 17 May 2010
Received in revised form 18 June 2010
Accepted 18 June 2010
Available online 25 June 2010

Keywords:
Optical chemical sensor
Optode
Mathematical modeling
Flow injection analysis
Determination of copper

ABSTRACT

A general mathematical model of a flow-through optical chemical sensor prepared by the immobilization of 1-(2′-pyridylazo)-2-naphthol (PAN) into a commercial Nafion® membrane was developed. The model takes into account the preparation of the optode membrane and in our opinion the most important chemical and physical processes involved in the generation of the analytical signal. The following model parameters were determined separately from the experimental verification of the model: aqueous diffusion coefficient of $CuSO_4$ – 8.75×10^{-10} m^2 s^{-1}; membrane self-diffusion coefficient of the Cu^{2+}–PAN complex and Cu^{2+} – 1.87×10^{-16} and 6.00×10^{-15} m^2 s^{-1}, respectively; Nafion/water ion-exchange equilibrium constants for the Cu^{2+}–PAN complex and Cu^{2+} – 109.2 and 3.65×10^{-3}, respectively. Very good agreement was obtained between the experimental optode response and the model predictions thus showing that the model developed could be used successfully for the mathematical description and optimization of the PAN/Nafion optode as well as of other ion-exchange membrane based optodes having a similar response mechanism.

1. Introduction

Nafion® is a perfluorosulfonated ion-exchange polymer which is widely used in analytical practice for the preparation of electrochemical sensors [1–3]. It is optically transparent and has a very high mechanical and chemical stability. All these properties make this polymer very suitable for the construction of optical chemical sensors by immobilizing appropriate reagents. A Nafion optode developed earlier by the immobilization of tris(1,10-phenanthroline)iron(II) (Ferroin) was successfully used for the detection of ascorbic acid in pharmaceuticals [4,5]. The response mechanism of this optode involved the reduction of the blue colored Ferriin complex (tris(1,10-phenanthroline)iron(III)) to the red colored Ferroin complex. Another redox Nafion based optode for the indirect determination of SeO_3^{2-} was constructed by the immobilization of p-amino-p′-methoxydiphenylamine (Variamine Blue) [6]. The sensing mechanism in this case involved the formation of a violet colored species in the Nafion membrane as a result of the oxidation of Variamine Blue by iodine produced in the reaction between iodide and selenite in solution. The immobilization of methyl violet in Nafion produced an optode membrane which changed color in the pH range from 0.6 to 3.0 [7]. Nafion based optodes for the detection of the metal ions Ni^{2+}, Cu^{2+} and Hg^{2+} were developed by the immobilization of the colorimetric chelators 1-(2′-pyridylazo)-2-naphthol (PAN) [8–10], its derivative 4-decyloxy-2-(2-pyridylazo)-1-naphthol (DPAN) [11], diphenyl-carbazone [12], and 2-(5-bromo-2-pyridylazo)-5-(diethylamino)phenol [13]. A separate study reported on the composition of the violet colored Cu^{2+}–PAN complex observed in PAN/Nafion membranes as CuL^+ where L is deprotonated PAN [14].

The development of an adequate mathematical model of the Nafion based optodes mentioned above will give not only a better insight into their response mechanism but will also help to improve their design and performance (e.g. selectivity, sensitivity and response time).

Flow injection (FI) systems are very suitable for studying the dynamic behavior of chemical sensors because they allow the generation of a reproducible transient concentration profile of the detected chemical species at the sensor/solution interface [15,16].

The present paper reports on the development of a general mathematical model of the Nafion optode incorporating PAN in the case of Cu^{2+} determination and the experimental verification of this model under FI conditions. The experimental determination of the model parameters (e.g. diffusion coefficients, equilibrium constants, molar absorptivities) whose numerical values were not available in the literature is also outlined.

* Corresponding author. Tel.: +61 3 8344 7931; fax: +61 3 9347 5180.
E-mail address: s.kolev@unimelb.edu.au (S.D. Kolev).

0039-9140/$ – see front matter © 2010 Elsevier B.V. All rights reserved.
doi:10.1016/j.talanta.2010.06.027

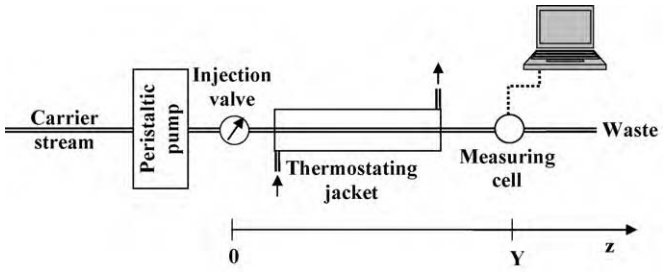

Fig. 1. Schematic of the experimental FI system.

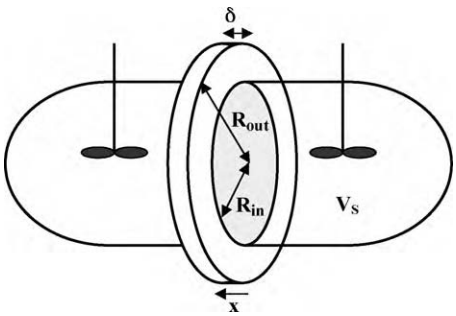

Fig. 2. Schematic of the experimental extraction system (V_S is solution volume, δ is the thickness of the membrane, R_{in} and R_{out} are the radius of the membrane exposed to the solution and the total radius, respectively).

2. Theory

2.1. Determination of the diffusion coefficient of $CuSO_4$ in aqueous solutions

The dispersion of $CuSO_4$ in the experimental FI system (Fig. 1) was described mathematically by the axially dispersed plug flow model (Eq. (1)) [17].

$$\frac{\partial c}{\partial t} = D_L \frac{\partial^2 c}{\partial z^2} - u\frac{\partial c}{\partial z} \tag{1}$$

where c is the concentration of $CuSO_4$, z is the axial distance, u is the average linear flow velocity and D_L is the axial-dispersion coefficient which in the general case is an empirical parameter analogous to the molecular diffusion coefficient in Fick's laws.

All flow-through sections of the experimental FI system had equal diameters and the volumes of the measuring cell and the injection loop were much smaller than the reactor volume. Under these conditions it was possible to view the FI system as a single tubular reactor of length Y and to neglect the so-called end effects [18]. In this case the analytical solution of Eq. (1) for $z = Y$ is [19]:

$$c(Y,t) = \frac{1}{2}\left\{\mathrm{erf}\left[\frac{uY - Y}{2(tD_L)^{1/2}}\right] + \mathrm{erf}\left[\frac{Y + \alpha - ut}{2(tD_L)^{1/2}}\right]\right\} \tag{2}$$

where erf is the error function and α is the sample volume divided by the volumetric flow rate.

The axial-dispersion coefficient (D_L) was determined by fitting Eq. (2) to the experimental FI transient concentration curves.

The experimental conditions (i.e. flow rate and reactor length) were selected such that the overall dispersion process in the reactor was controlled mainly by molecular diffusion. In this case, the mean residence time reduced to molecular diffusion scale (i.e. the Fourier number, Eq. (3)) was greater than 0.7 and Taylor's theory could be applied to calculate the axial-dispersion coefficient [19–21].

$$D_L = \frac{uY}{48\tau} \tag{3}$$

where $\tau = D_m Y/ua^2$, a is the reactor diameter and D_m is the diffusion coefficient of the solute.

2.2. Determination of the diffusion coefficients and the ion-exchange equilibrium constants of Cu^{2+} and CuL^+ in Nafion membranes in their Na^+ form

A mathematical model similar to the one reported earlier [22,23] was used to describe the overall membrane extraction process. This model takes into account the ion-exchange equilibria at the membrane–solution interface (Eqs. (4a) and (4b)) and the coupled diffusion of Cu^{2+} and CuL^+ within the Nafion membrane (Eq. (5)). In the case of CuL^+ extraction, the Nafion membrane was in its Na^+ form while Cu^{2+} was extracted into Nafion in its H^+ form.

$$CuL^+(s) + Na^+(m) \rightleftharpoons CuL^+(m) + Na^+(s) \qquad K_{CuL^+/Na^+} = \frac{c^m_{CuL^+} c^s_{Na^+}}{c^s_{CuL^+} c^m_{Na^+}} \tag{4a}$$

$$Cu^{2+}(s) + 2H^+(m) \rightleftharpoons Cu^{2+}(m) + 2H^+(s) \qquad K_{Cu^{2+}/H^+} = \frac{c^m_{Cu^{2+}} \left(c^s_{H^+}\right)^2}{c^s_{Cu^{2+}} \left(c^m_{H^+}\right)^2} \tag{4b}$$

where m and s refer to membrane and solution, respectively.

$$\frac{\partial c^m_{Z^{n+}}}{\partial t} = \overline{D}\left\{\frac{1}{r}\frac{\partial c^m_{Z^{n+}}}{\partial r} + \frac{\partial^2 c^m_{Z^{n+}}}{\partial r^2} + \frac{\partial^2 c^m_{Z^{n+}}}{\partial x^2}\right\} + \overline{F}\left\{\left(\frac{\partial c^m_{Z^{n+}}}{\partial r}\right)^2 + \left(\frac{\partial c^m_{Z^{n+}}}{\partial x}\right)^2\right\} \tag{5}$$

where x and r are the axial and the radial distance (Fig. 2) and $c^m_{Z^{n+}}$ is the concentration of the extracted species Z^{n+} (Cu^{2+} or CuL^+) within the membrane. The interdiffusion coefficient ($\overline{D}$) and the coefficient $\overline{F}$ are defined by the following expressions [24]:

For the extraction of CuL^+ into Nafion in its Na^+ form ($n = 1$):

$$\overline{D} = \frac{D_{Na^+} D_{CuL^+} c^m_{Na^+,0}}{D_{Na^+} c^m_{Na^+,0} + \left(D_{CuL^+} - D_{Na^+}\right) c^m_{CuL^+}} \tag{5a}$$

$$\overline{F} = \frac{\left(D_{Na^+} - D_{CuL^+}\right) D_{Na^+} D_{CuL^+} c^m_{Na^+,0}}{\left[D_{Na^+} c^m_{Na^+,0} + \left(D_{CuL^+} - D_{Na^+}\right) c^m_{CuL^+}\right]^2} \tag{5b}$$

For the extraction of Cu^{2+} into Nafion in its H^+ form ($n = 2$):

$$\overline{D} = \frac{D_{H^+} D_{Cu^{2+}} \left(c^m_{H^+,0} + 2c^m_{Cu^{2+}}\right)}{D_{H^+} c^m_{H^+,0} + 2\left(2D_{Cu^{2+}} - D_{H^+}\right) c^m_{Cu^{2+}}} \tag{5c}$$

$$\overline{F} = \frac{4\left(D_{H^+} - D_{Cu^{2+}}\right) D_{H^+} D_{Cu^{2+}} c^m_{H^+,0}}{\left[D_{H^+} c^m_{H^+,0} + 2\left(2D_{Cu^{2+}} - D_{H^+}\right) c^m_{Cu^{2+}}\right]^2} \tag{5d}$$

where subscript 0 refers to the initial concentration.

The initial and boundary conditions of Eq. (5) are:

$$c^m_{Z^{n+}}(0,x,r) = 0 \tag{6a}$$

$$\left(\frac{\partial c^m_{Z^{n+}}}{\partial x}\right)_{x=0, R_{in} < r \le R_{out}} = 0 \tag{6b}$$

$$\left(\frac{\partial c^{m}_{Z^{n+}}}{\partial x}\right)_{x=\delta/2} = 0 \quad (6c)$$

$$\left(\frac{\partial c^{m}_{Z^{n+}}}{\partial r}\right)_{r=0} = 0 \quad (6d)$$

$$\left(\frac{\partial c^{m}_{Z^{n+}}}{\partial r}\right)_{r=R_{out}} = 0 \quad (6e)$$

where δ is the thickness of the membrane, R_{in} and R_{out} are the radius of the membrane exposed to the solution and the total radius, respectively (Fig. 2).

The interfacial concentration of Z^{n+} can be defined by the following expressions:

For the extraction of CuL^{+} into Nafion in its Na^{+} form ($n = 1$):

$$c^{m}_{CuL^{+}}(t, 0, r \le R_{in}) = \frac{K_{CuL^{+}/Na^{+}} c^{s}_{CuL^{+}} c^{m}_{Na^{+},0}}{c^{s}_{Na^{+},0} + c^{s}_{CuL^{+},0} + c^{s}_{CuL^{+}} \left(K_{CuL^{+}/Na^{+}} - 1\right)} \quad (7)$$

For the extraction of Cu^{2+} into Nafion in its H^{+} form ($n = 2$):

$$c^{m}_{Cu^{2+}}(t, 0, r \le R_{in}) = \frac{1}{2}\left\{-a - \sqrt{a^2 - 4b}\right\} \quad (8)$$

where

$$a = -\left\{c^{m}_{H^{+},0} + \frac{\left(0.5c^{s}_{H^{+},0} + c^{s}_{Cu^{2+},0} - c^{s}_{Cu^{2+}}\right)^2}{K_{Cu^{2+}/H^{+}} c^{s}_{Cu^{2+}}}\right\} \quad (8a)$$

$$b = \left(0.5c^{m}_{H^{+},0}\right)^2 \quad (8b)$$

The concentration of Z^{n+} in the solution ($c^{s}_{Z^{n+}}$) can be determined from the mass-balance of Z^{n+} in the extraction cell [23], i.e.

$$c^{s}_{Z^{n+}} = c^{s}_{Z^{n+},0} - 2\frac{\pi}{V_s}\int_0^{R_{out}}\left\{r\int_0^{\delta/2} c^{m}_{Z^{n+}} dx\right\} dr \quad (9)$$

where V_s is the volume of the solution.

The numerical procedure based on the implicit finite difference method and the implicit alternating-direction finite difference method, utilized in solving the model, is outlined elsewhere [22,23].

2.3. Development of the mathematical model

The sensing mechanism of the optode involves the mass-transfer of Cu^{2+} ions across the membrane/solution interface into the membrane where they react with LH to form the violet colored CuL^{+} complex. This reaction is accompanied by the release of H^{+} ions which can protonate LH in the membrane to form another chemical species absorbing in the visible range (LH_2^{+}). The total absorbance of the membrane is equal to the sum of the absorbances of the chemical species mentioned above:

$$A = \delta\left\{\varepsilon_{LH}\overline{c^{m}_{LH}} + \varepsilon_{LH_2^{+}}\overline{c^{m}_{LH_2^{+}}} + \varepsilon_{CuL^{+}}\overline{c^{m}_{CuL^{+}}}\right\} \quad (10)$$

where ε_i and $\overline{c_i^{m}}$ are the molar absorptivity and the average concentration of the i-th absorbing chemical species (Eq. (10a)), respectively.

$$\overline{c_i^{m}} = \frac{1}{\delta}\int_0^{\delta} c_i^{m} dx \quad (10a)$$

The initial distribution of LH within the optode membrane prior to Cu^{2+} measurements was calculated by the mathematical model [23] developed earlier by us for the extraction of LH into Nafion membranes.

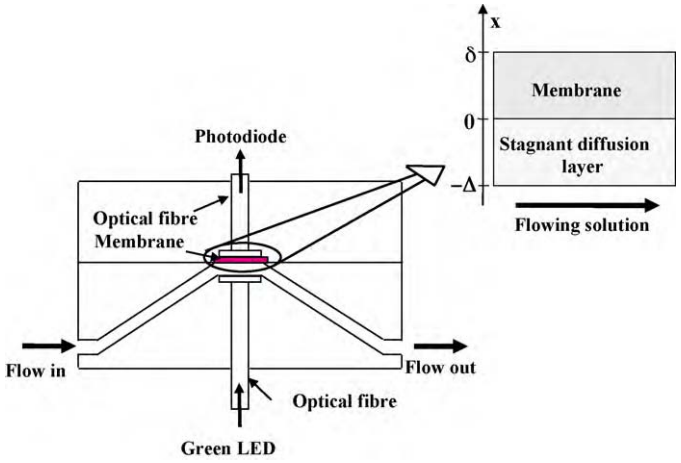

Fig. 3. Schematic of the optode flow-through measuring cell.

The mathematical model of the FI system (Fig. 1) incorporating the optode flow-through measuring cell (Fig. 3) consists of the mathematical descriptions of the following physicochemical subsystems: (1) mass-transfer of the Cu^{2+} ions in the aqueous solution towards the optode membrane; (2) mass-transfer of the Cu^{2+} ions and other mobile chemical species within the optode membrane; (3) ion-exchange at the membrane/solution interface; (4) protonation and complexation reactions within the optode membrane. The mathematical descriptions of these four interrelated subsystems are outlined in the following paragraphs.

2.3.1. Mass-transfer of the Cu^{2+} ions in the aqueous solution towards the membrane

It was assumed that a stagnant diffusion layer of thickness Δ separated the flowing carrier solution from the optode membrane (Fig. 3) and that the concentration of the Cu^{2+} cation at the flowing solution/stagnant layer interface was uniform. This assumption allowed to describe the mass-transport of Cu^{2+} through the stagnant diffusion layer as one-dimensional Fickian diffusion (Eq. (11)).

$$\frac{\partial c^{s}_{Cu^{2+}}}{\partial t} = D_{Cu^{2+}}\frac{\partial c^{m}_{Cu^{2+}}}{\partial x^2} \quad (11)$$

The initial and boundary conditions of Eq. (11) are:

$$c^{s}_{Cu^{2+}}(x, 0) = 0 \quad (11a)$$

$$c^{s}_{Cu^{2+}}(-\Delta, t) = c(Y, t) \quad (11b)$$

$$c^{s}_{Cu^{2+}}(0, t) = c^{s,eq}_{Cu^{2+}}(0, t) \quad (11c)$$

where $c(Y,t)$ can be calculated by Eq. (2) and $c^{s,eq}_{Cu^{2+}}(0, t)$ is the equilibrium interfacial concentration of Cu^{2+} on the solution side of the membrane/solution interface.

The concentrations of the H^{+} and Na^{+} ions within the stagnant diffusion layer were assumed to be constant and equal to those in the carrier solution.

2.3.2. Mass-transfer of Cu^{2+} and other chemical species within the optode membrane

By comparing the membrane self-diffusion coefficients of the chemical species involved in the optode sensing mechanism determined in this ($D_{Cu^{2+}} = 6.00 \times 10^{-15}\,m^2\,s^{-1}$; $D_{CuL^{+}} = 1.87 \times 10^{-16}\,m^2\,s^{-1}$) and earlier ($D_{H^{+}} = 1.35 \times 10^{-10}\,m^2\,s^{-1}$ and $D_{Na^{+}} = 1.02 \times 10^{-10}\,m^2\,s^{-1}$ [24]; $D_{LH_2^{+}} = 4.00 \times 10^{-16}\,m^2\,s^{-1}$ [23]) studies, it was concluded that in the time scale of the optode measurements

LH, LH_2^+ and the CuL^+ complex could be considered as immobile. The model takes into account the diffusion of Cu^{2+}, Na^+ and H^+ ions only. It should be noted that the self-diffusion coefficient of Cu^{2+} is only an order of magnitude higher than that of PAN. The difference between the actual interdiffusion coefficients (Eqs. (5a) and (5c)), which determine the actual mass-transfer rates, is greater because of the higher charge of the Cu^{2+} ion. The diffusion of the three mobile cations within the ion-exchange membrane is coupled through the Nernst–Planck equation, the electroneutrality requirement and the zero-current condition. The corresponding fluxes can be described by the following equations [25]:

$$\Phi^{m}_{H^+} = -D_{H^+}\left\{\frac{\partial c^{m}_{H^+}}{\partial x} - c^{m}_{H^+}\Psi\right\} \tag{12a}$$

$$\Phi^{m}_{Cu^{2+}} = -D_{Cu^{2+}}\left\{\frac{\partial c^{m}_{Cu^{2+}}}{\partial x} - 2c^{m}_{Cu^{2+}}\Psi\right\} \tag{12b}$$

$$\Phi^{m}_{Na^+} = -\Phi^{m}_{H^+} - 2\Phi^{m}_{Cu^{2+}} \tag{12c}$$

where Ψ is defined as [25]:

$$\Psi = \frac{D_{H^+}\left(\partial c^{m}_{H^+}/\partial x\right) + D_{Na^+}\left(\partial c^{m}_{Na^+}/\partial x\right) + 2D_{Cu^{2+}}\left(\partial c^{m}_{Cu^{2+}}/\partial x\right)}{D_{H^+}c^{m}_{H^+} + D_{Na^+}c^{m}_{Na^+} + 4D_{Cu^{2+}}c^{m}_{Cu^{2+}}} \tag{13}$$

The equations describing the coupled diffusion of Cu^{2+}, Na^+ and H^+ (Eqs. (15)–(17)) can be derived by substituting Eqs. (12a)–(12c) into the equation of continuity (Eq. (14)).

$$\frac{\partial c}{\partial t} = -\frac{\partial \Phi}{\partial x} \tag{14}$$

$$\frac{\partial c^{m}_{Cu^{2+}}}{\partial t} = \frac{\partial}{\partial x}\left[\left(\frac{\alpha_{Cu^{2+}}}{\gamma}\right)\frac{\partial c^{m}_{H^+}}{\partial x}\right] + \frac{\partial}{\partial x}\left[\left(\frac{\beta_{Cu^{2+}}}{\gamma}\right)\frac{\partial c^{m}_{Cu^{2+}}}{\partial x}\right] \tag{15}$$

$$\frac{\partial c^{m}_{H^+}}{\partial t} = \frac{\partial}{\partial x}\left[\left(\frac{\alpha_{H^+}}{\gamma}\right)\frac{\partial c^{m}_{H^+}}{\partial x}\right] + \frac{\partial}{\partial x}\left[\left(\frac{\beta_{H^+}}{\gamma}\right)\frac{\partial c^{m}_{Cu^{2+}}}{\partial x}\right] \tag{16}$$

$$c^{m}_{Na^+} = c^{m}_{0} - c^{m}_{H^+} - 2c^{m}_{Cu^{2+}} \tag{17}$$

where

$$\alpha_{Cu^{2+}} = 2c^{m}_{Cu^{2+}}D_{H^+}D_{Cu^{2+}}\left(1 - \frac{D_{Na^+}}{D_{H^+}}\right) \tag{18a}$$

$$\beta_{Cu^{2+}} = -c^{m}_{H^+}D_{H^+}D_{Cu^{2+}} - 4c^{m}_{Cu^{2+}}D_{Na^+}D_{Cu^{2+}}\left(1 - \frac{c^{m}_{Na^+}}{4c^{m}_{Cu^{2+}}}\right) \tag{18b}$$

$$\alpha_{H^+} = -4c^{m}_{Cu^{2+}}D_{H^+}D_{Cu^{2+}} - c^{m}_{H^+}D_{H^+}D_{Na^+}\left(1 - \frac{c^{m}_{Na^+}}{c^{m}_{H^+}}\right) \tag{18c}$$

$$\beta_{H^+} = 2c^{m}_{H^+}D_{H^+}D_{Cu^{2+}}\left(1 - \frac{c^{m}_{Na^+}}{4c^{m}_{Cu^{2+}}}\right) \tag{18d}$$

$$\gamma = c^{m}_{H^+}D_{H^+} + 4c^{m}_{Cu^{2+}}D_{Cu^{2+}} + c^{m}_{Na^+}D_{Na^+} \tag{18e}$$

The total equivalent concentration of the mobile cations in the membrane (c^{m}_{0}, Eq. (19)) is time and position dependent because of the simultaneously occurring mass-transfer and Cu^{2+}/LH complexation processes. It is related to the constant concentration of the ion-exchange sites in the membrane ($c^{m}_{Na^+,0}$) and the transient concentrations of LH_2^+ and CuL^+, assumed as immobile ions.

$$c^{m}_{0} = c^{m}_{Na^+,0} - c^{m}_{LH_2^+} - c^{m}_{CuL^+} \tag{19}$$

The initial and boundary conditions of Eqs. (15) and (16) are:

$$c^{m}_{Cu^{2+}}(x, 0) = 0 \tag{20a}$$

$$c^{m}_{H^+}(x, 0) = 0 \tag{20b}$$

$$c^{m}_{Cu^{2+}}(0, t) = c^{m,eq}_{Cu^{2+}}(0, t) \tag{20c}$$

$$c^{m}_{H^+}(0, t) = c^{m,eq}_{H^+}(0, t) \tag{20d}$$

$$\left(\frac{\partial c^{m}_{Cu^{2+}}}{\partial x}\right)_{x=\delta} = 0 \tag{20e}$$

$$\left(\frac{\partial c^{m}_{H^+}}{\partial x}\right)_{x=\delta} = 0 \tag{20f}$$

where $c^{m,eq}_{Cu^{2+}}(0, t)$ and $c^{m,eq}_{H^+}(0, t)$ are the equilibrium interfacial concentrations of Cu^{2+} and H^+ on the membrane side of the membrane/solution interface.

2.3.3. Ion-exchange at the membrane/solution interface

It was assumed that all ion-exchange equilibria at the membrane/solution interface (Eqs. (4b) and (21)) took place instantaneously.

$$Cu^{2+}(s) + 2Na^+(m) \rightleftharpoons Cu^{2+}(m) + 2Na^+(s)$$

$$K_{Cu^{2+}/Na^+} = \frac{c^{m}_{Cu^{2+}}\left(c^{s}_{Na^+}\right)^2}{c^{s}_{Cu^{2+}}\left(c^{m}_{Na^+}\right)^2} \tag{21}$$

The equilibrium interfacial concentrations of Cu^{2+}, Na^+ and H^+ at $x = \delta$ both in the membrane and in the solution (Fig. 3) were described by combining the expressions for the ion-exchange equilibria at the membrane/solution interface (Eqs. (4b) and (21)), the mass-balance equation for Cu^{2+} (Eq. (22)) and the electroneutrality condition with respect to the mobile ions within the membrane (Eq. (19)).

$$\overline{c_{Cu^{2+}}(0, t)} = c^{m}_{Cu^{2+}}(0, t) + c^{s}_{Cu^{2+}}(0, t) \tag{22}$$

where $\overline{c_{Cu^{2+}}(0, t)}$ is the total concentration of free Cu^{2+} at the membrane/solution interface.

By combining Eqs. (4b) and (21) and taking into account the assumption made earlier that the concentrations of the Na^+ ($c^{s}_{Na^+}$) and H^+ ($c^{s}_{H^+}$) ions in the stagnant diffusion layer (Fig. 3) are constant, the following relationship between $c^{m}_{Na^+}(0, t)$ and $c^{m}_{H^+}(0, t)$ was derived:

$$c^{m}_{Na^+}(0, t) = \Psi c^{m}_{H^+}(0, t) \tag{23}$$

where

$$\Psi = \sqrt{\frac{K^{*}_{Cu^{2+}/H^+}}{K^{*}_{Cu^{2+}/Na^+}}} \tag{24}$$

$$K^{*}_{Cu^{2+}/H^+} = \frac{K_{Cu^{2+}/H^+}}{\left(c^{s}_{H^+}\right)^2} \tag{25}$$

$$K^{*}_{Cu^{2+}/Na^+} = \frac{K_{Cu^{2+}/Na^+}}{\left(c^{s}_{Na^+}\right)^2} \tag{26}$$

By substituting the expression for $c^{m}_{Na^+}(0, t)$ (Eq. (23)) in Eq. (15) the following equation was obtained:

$$c^{m}_{Cu^{2+}}(0, t) = 0.5\left\{c^{m}_{0} - [1 + \Psi]c^{m}_{H^+}(0, t)\right\} \tag{27}$$

The combining of Eqs. (22), (25) and (27) resulted in a cubic equation (Eq. (28)) with respect to the equilibrium interfacial membrane concentration of the H^+ ion, $c^{m,eq}_{H^+}(0, t)$. This equation was solved by Cardano's formula [26] and the equilibrium interfacial membrane concentrations of Na^+ ($c^{m,eq}_{Na^+}(0, t)$) and Cu^{2+} ($c^{m,eq}_{Cu^{2+}}(0, t)$) on the one hand and the interfacial solution concentration of Cu^{2+} ($c^{s,eq}_{Cu^{2+}}(0, t)$), on the other, were calculated by Eqs. (23), (27) and (22), respectively.

$$\left[c^{m,eq}_{H^+}(0, t)\right]^3 + \frac{2\overline{c_{Cu^{2+}}(0, t)} - c^{m}_{0}}{1 + \Psi}\left[c^{m,eq}_{H^+}(0, t)\right]^2$$

$$+\frac{1}{K^{*}_{Cu^{2+}/H^{+}}}\left[c^{m,eq}_{H^{+}}(0,t)\right]-\frac{c^{m}_{0}}{K^{*}_{Cu^{2+}/H^{+}}(1+\Psi)}=0 \quad (28)$$

2.3.4. Protonation and complexation reactions within the optode membrane

It was assumed that the protonation (Eq. (29)) and complexation (Eq. (30)) equilibria within the membrane, similarly to the ion-exchange equilibria outlined earlier, were established instantaneously.

$$LH_2^{+} \rightleftharpoons LH + H^{+} \qquad K_a=\frac{c^{m}_{LH}c^{m}_{H^{+}}}{c^{m}_{LH_2^{+}}} \quad (29)$$

$$Cu^{2+} + LH \rightleftharpoons CuL^{+} + H^{+} \qquad K_f=\frac{c^{m}_{CuL^{+}}c^{m}_{H^{+}}}{c^{m}_{Cu^{2+}}c^{m}_{LH}} \quad (30)$$

where K_a is the acidity constant of LH^+ and K_f is the formation constant of CuL^+.

The unknown concentrations of LH, LH_2^+, CuL^+, H^+, and Cu^{2+} in Eqs. (29) and (30) are also interrelated through the mass-balance equations for LH (Eq. (31)) and Cu^{2+} (Eq. (32)) and the condition of electroneutrality (Eq. (33)).

$$\overline{c_{LH}}=c^{m}_{LH}+c^{m}_{LH_2^{+}}+c^{m}_{CuL^{+}} \quad (31)$$

$$\overline{c^{m}_{Cu^{2+}}}=c^{m}_{Cu^{2+}}+c^{m}_{CuL^{+}} \quad (32)$$

$$2c^{m}_{Cu^{2+}}+c^{m}_{LH_2^{+}}+c^{m}_{CuL^{+}}+c^{m}_{H^{+}}=\text{const} \quad (33)$$

where $\overline{c_{LH}}$ and $\overline{c^{m}_{Cu^{2+}}}$ are the total concentrations of LH and Cu^{2+} in the membrane, respectively.

A quadratic equation with respect to c^{m}_{LH} was derived. An analytical [26] and a numerical method (Bearstow's method [27]) were attempted to solve this equation. In both cases the solution obtained was unstable. For this reason an iterative approach was developed for solving Eqs. (29)–(33).

In this approach the protonation of PAN (Eq. (29)) was regarded as independent from the complexation reaction between PAN and Cu^{2+} (Eq. (30)). This allowed the calculation of the unknown concentrations mentioned above at each iterative step in two subsequent sub-steps. In the first sub-step the complexation process (Eq. (30)) was completely neglected and the unknown concentrations of LH, LH_2^+ and H^+ in Eq. (29) were assumed as interrelated through the simplified equations for the mass-balance of PAN (Eq. (34)) and the simplified condition of electroneutrality (Eq. (35)).

$$\overline{c^{*}_{LH}}=c^{m}_{LH}+c^{m}_{LH_2^{+}} \quad (34)$$

$$\overline{c^{*}_{charge}}=c^{m}_{H^{+}}+c^{m}_{LH_2^{+}} \quad (35)$$

where $\overline{c^{*}_{LH}}$ and $\overline{c^{*}_{charge}}$ are the total concentration of PAN (excluding CuL^+) and the total positive charge (excluding the positive charge of the Cu^{2+} and CuL^+ ions), respectively.

The solution of the resulting quadratic equation (Eq. (36)) allowed the calculation of the equilibrium concentration of LH_2^+.

$$c^{m}_{LH_2^{+}}=\frac{1}{2}\left\{\overline{c^{*}_{charge}}+\overline{c^{*}_{LH}}+K_a-\sqrt{\left(\overline{c^{*}_{charge}}+\overline{c^{*}_{LH}}+K_a\right)^{2}-4\overline{c^{*}_{charge}}\,\overline{c^{*}_{LH}}}\right\} \quad (36)$$

In the second sub-step, focusing on the formation of the complex CuL^+ (Eq. (30)), the protonation of PAN (Eq. (29)) was completely neglected. The unknown concentrations in Eq. (30) were also related through the corresponding simplified mass-balance equations for PAN (Eq. (37)) and Cu^{2+} (Eq. (38)) and the simplified electroneutrality condition (Eq. (39)).

$$\overline{c^{**}_{LH}}=c^{m}_{LH}+c^{m}_{CuL^{+}} \quad (37)$$

$$\overline{c^{**}_{Cu^{2+}}}=c^{m}_{Cu^{2+}}+c^{m}_{CuL^{+}} \quad (38)$$

$$\overline{c^{**}_{charge}}=c^{m}_{H^{+}}+c^{m}_{CuL^{+}}+2c^{m}_{Cu^{2+}} \quad (39)$$

where $\overline{c^{**}_{LH}}$, $\overline{c^{*}_{Cu^{2+}}}$ and $\overline{c^{**}_{charge}}$ are the total concentration of PAN (excluding LH_2^+) and Cu^{2+} and the total positive charge (excluding the positive charge of the LH_2^+ ion), respectively.

A quadratic equation (Eq. (40)) with respect to the concentration of the complex CuL^+ was derived on the basis of Eqs. (30) and (37)–(39).

$$c^{m}_{CuL^{+}}=\frac{1}{2}\left\{-a-\sqrt{a^{2}-4b}\right\} \quad (40)$$

where

$$a=-\frac{\overline{c^{**}_{charge}}+2\overline{c^{**}_{Cu^{2+}}}+K_f\left(\overline{c^{**}_{Cu^{2+}}}+\overline{c^{**}_{LH}}\right)}{K_f-1} \quad (40a)$$

$$b=\frac{K_f\overline{c^{**}_{Cu^{2+}}}\,\overline{c^{**}_{LH}}}{K_f-1} \quad (40b)$$

The concentrations of the other chemical species participating in the complexation reaction (LH, Cu^{2+} and H^+) were calculated using Eqs. (37)–(39). The values of $c^{m}_{H^{+}}$ and c^{m}_{LH} together with the value of $c^{m}_{LH_2^{+}}$ determined previously (Eq. (36)) were used to calculate the function (Eq. (41)) minimized in the iteration procedure.

$$Q=\text{abs}\left\{\frac{1-\left(c^{m}_{LH}c^{m}_{H^{+}}/c^{m}_{LH_2^{+}}\right)}{K_a}\right\} \quad (41)$$

It was assumed that if Q was less than 1×10^{-3} the calculated concentrations of the chemical species participating in the protonation and the complexation reactions could be considered as reasonably close to the actual equilibrium values. Otherwise, the iteration procedure (Eqs. (34)–(41)) was repeated. The iterative approach outlined above was found to be stable and rapidly converging.

2.4. Numerical solution of the model

The mathematical model outlined above was numerically solved to calculate the theoretical transient absorbance curves (Eq. (10)). An explicit finite difference scheme [28] was employed for solving the mass-transport partial differential equations (Eqs. (11), (15) and (16)). At each time increment the concentration of Cu^{2+} in the flowing solution at $z=Y$ (Eq. (2)) and in the stagnant layer at $x=0$ (Fig. 3) was calculated (Eq. (11)). The next step involved the calculation of the equilibrium interfacial concentrations of Cu^{2+}, Na^+ and H^+. After this step, the coupled diffusion step was implemented (Eqs. (16)–(18)), followed by calculating the equilibrium concentrations of Cu^{2+}, H^+, LH, LH_2^+ and CuL^+ by the iterative procedure outlined above. Finally, the total absorbance of the membrane (Eq. (10)) was calculated. A computer program in Quick C® (Microsoft) implementing the algorithm outlined above was developed.

The values of the acidity constant of LH_2^+ (K_a) [29] and the formation constant of CuL^+ (K_f) [14] used in the calculations were 4.467×10^{-4} mol L^{-1} and 8.059×10^{4}, respectively. The concentration of the ion-exchange sites in the membrane ($c^{m}_{Na^{+},0}$) at equilibrium with water was calculated as equal to 1.503 mol L^{-1} on the basis of the membrane ion-exchange capacity [23] (0.909 mequiv. g^{-1}), dry mass and volume after swelling.

3. Experimental

3.1. Reagents

The perfluorosulfonated ionomer membrane, Nafion® 117, was purchased from Aldrich. Analytical grade PAN (Fluka), absolute ethanol (Biolab Scientific, Australia), sodium acetate (Ajax Chemicals, Australia), sodium nitrate (Ajax Chemicals, Australia), $CuSO_4{\cdot}5H_2O$ (BDH, Australia) and nitric acid (Ajax Chemicals, Australia) were used as received. Deionized water (Barnstead, Dubuque, IA, higher than 17 MΩ cm) was used throughout the experiments.

3.2. Apparatus

The spectrophotometric measurements were performed with a Shimadzu UV-240 UV–visible spectrophotometer (Japan) with an OPI-2 interface and 10 mm cells. The thickness of the Nafion® membranes was measured by a calibrated microscope (Nikon Labophot 2, Type 104, Japan) with ± 0.005 mm accuracy. Flame atomic absorption spectrometric (AAS) measurements were carried out by a GBC Model 933 spectrometer (Australia).

3.3. FI system

The determination of the $CuSO_4$ diffusion coefficient was carried out in a single-channel FI system (Fig. 1) incorporating a peristaltic pump (Alitea C4, Sweden), a rotary injection valve (Model 5020, Rheodyne), Teflon tubing (i.d. 0.5 mm, Sigma–Aldrich), and a home-made flow-through measuring cell [8]. In the FI optode measurements, an electrically actuated and computer controlled multiposition selection valve (Model E10, Valco Instruments, USA) allowing switching between a carrier and several reagent solutions was inserted upstream of the peristaltic pump (Fig. 1). The length of the straight Teflon tube (referred to as the reactor) connecting the injection valve with the measuring cell (Fig. 1) was 2.01 m. The average internal diameter of the reactor (0.543 mm) and the sample volume (14.75 μL) were determined from the volume of deionized water which filled the corresponding tubing. The reservoir of the carrier solution was immersed in a water bath thermostated at 25 °C (Thermoregulator TH5, RATEK, Australia). Water from the water bath was also circulated constantly through the thermostating jacket of the reactor of the FI system (Fig. 1).

The volumetric flow rate was varied in the range from 0.200 to 0.600 mL min^{-1} and was measured before and after each experiment by collecting and weighing the effluent over 5 min.

The data acquisition and system control were performed by a PC with a PCL-818H data acquisition card (Advantech, Taiwan) running a program in C® (Microsoft) developed as part of this study.

The FI determination of the diffusion coefficient of $CuSO_4$ involved the use of a home-made conductimetric flow-through measuring cell described in detail elsewhere [31] and connected to a conductivity meter (Model 2100, TPS Pty Ltd, Australia). The home-made photometric flow-through measuring cell used in the optode experiments (Fig. 3) was equipped with a green LED (λ = 555 nm, Farnell Electronic Components, Australia) and a photodiode (SFH 250H, Siemens, Germany).

3.4. FI determination of the $CuSO_4$ diffusion coefficient in aqueous solutions

The conductimetric measuring cell was calibrated by continuously flowing 6 standard $CuSO_4$ solutions in the concentration range from 0 to 8.00×10^{-5} mol L^{-1}. The calibration curve was used to convert the FI transient conductivity curves into transient concentration curves for further processing. The FI experiments, carried out in triplicate, involved the injection of 14.75 μL of 1.00×10^{-3} mol L^{-1} $CuSO_4$ at three different flow rates (0.245, 0.369 and 0.522 mL min^{-1}).

3.5. Determination of the diffusion coefficient and the ion-exchange equilibrium constant of Cu^{2+} and the Cu^{2+}–PAN complex (CuL^+) in Nafion membranes in the Na^+ form

Extraction data required for the determination of the diffusion coefficients of Cu^{2+} and CuL^+ in Nafion and the corresponding ion-exchange equilibrium constants were obtained using an extraction system thermostated at 25 °C (Fig. 2) as used in earlier Nafion membrane studies [22,23]. This system consisted of two glass cells attached on both sides of a Nafion membrane, which had been pretreated with 5 mol L^{-1} nitric acid [23]. Nafion membranes in the Na^+ form were prepared by immersing the nitric acid pretreated membranes (H^+ form) into 1.0 mol L^{-1} $NaNO_3$ for 24 h. Prior to the extraction experiments, the Nafion membranes were allowed to equilibrate with the corresponding solvent to minimize effects caused by swelling of the membranes during extraction. The solutions in the two cells were mechanically stirred and the concentration of the extracted species (Cu^{2+} or CuL^+) was monitored. The concentration of Cu^{2+} was determined by flame AAS while that of the CuL^+ complex was measured spectrophotometrically at 550 nm corresponding to the absorption maximum of the complex. The copper extraction experiments were performed from aqueous solutions of $CuSO_4$ with concentrations 1.10×10^{-5} and 7.08×10^{-5} mol L^{-1}. Because of solubility problems, the CuL^+ complex was extracted into Nafion from ethanol–water solutions with ethanol concentrations 1.0, 3.0 and 4.0% (v/v). The corresponding initial concentrations of the complex in the ethanol–water solutions were 3.00×10^{-5}, 5.00×10^{-5} and 6.08×10^{-5} mol L^{-1}, respectively. The CuL^+ complex was obtained by mixing $CuSO_4$ and PAN in molar ratio 1:1 in the solvents mentioned above.

3.6. Preparation of the optode membranes

The optode membranes were prepared by extracting PAN (LH) into nitric acid pretreated Nafion membranes. This process involved immersing a membrane into 25 mL of a 5.00×10^{-5} mol L^{-1} solution of PAN in 40% (v/v) ethanol for 30 min. During this period PAN was immobilized into the membrane in its protonated form (LH_2^+) [23]. The membrane was subsequently transferred and stored in a 4.00 mol L^{-1} aqueous sodium acetate solution where the protons in the membrane were exchanged with sodium ions thus converting LH_2^+ to LH. Square pieces of the neutralized optode membrane were cut and incorporated into the flow-through photometric measuring cell.

3.7. Determination of the molar absorptivities of LH, LH_2^+ and CuL^+ in Nafion membranes

Nafion membranes (5 × 5 mm) with known concentrations of LH (7.844×10^{-4} mol L^{-1}), the CuL^+ complex (1.780×10^{-3} mol L^{-1}) and LH_2^+ (8.954×10^{-4} mol L^{-1}) were prepared according to the procedure outlined above. The first two membranes were prepared using Nafion in its Na^+ form while the third one was in its H^+ form. The membrane concentration of each of the colored chemical species mentioned above was calculated from the difference between its concentrations in the solution before and after the extraction had taken place. The membrane thickness (0.175 ± 0.005 mm) was considered as the optical path length. The absorbance measurements were conducted in the optode flow-through measuring cell against a blank Nafion membrane in its H^+ or Na^+ form.

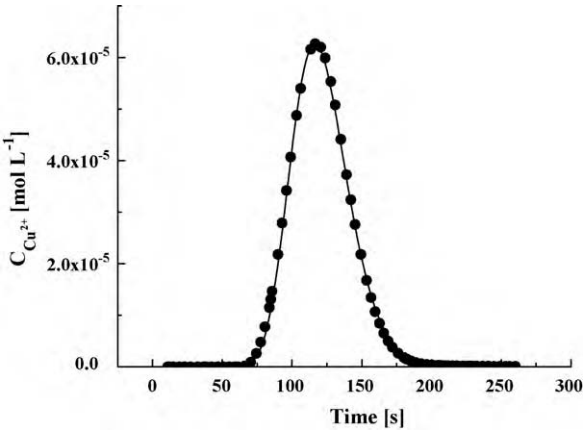

Fig. 4. Model predictions (—) that best fit the experimental FI transient $CuSO_4$ concentration data (●) (flow rate = 0.245 mL min^{-1}, sample volume = 14.75 μL).

3.8. FI experiments with optode detection

Standard solutions of $CuSO_4$ in the concentration range from 2.90×10^{-4} to 1.37×10^{-3} mol L^{-1} were injected into a deionized water carrier stream flowing at 0.306 mL min^{-1}. When the transient absorbance curve reached a pseudo steady-state value the optode membrane was regenerated by sequentially flowing 2.00 mol L^{-1} HCl solution for 20 s, deionized water for 10 s and 4.00 mol L^{-1} sodium acetate for 300 s.

4. Results and discussion

4.1. Determination of the diffusion coefficient of $CuSO_4$ in aqueous solutions

The repeatability of the FI experiments involving the injection of standard $CuSO_4$ solutions into a carrier stream of deionized water (Fig. 1) was excellent since the concentration curves monitored at the same flow rate were almost indistinguishable from each other. The excellent agreement between the experimental concentration curves and the model predictions that best fit them is illustrated in Fig. 4. The diffusion coefficient of $CuSO_4$ (D_m) obtained at 25 °C and flow rates of 0.245, 0.369 and 0.522 mL min^{-1} was 8.71×10^{-10}, 8.78×10^{-10} and 8.76×10^{-10} m^2 s^{-1}, respectively, with an average value of 8.75×10^{-10} m^2 s^{-1}.

4.2. Determination of the diffusion coefficients and the ion-exchange equilibrium constants of Cu^{2+} and CuL^+ in Nafion membranes in their Na^+ form

The self-diffusion coefficients and the ion-exchange equilibrium constants of cations Cu^{2+} and CuL^+ were determined by fitting the model to the experimental extraction data. Fig. 5 illustrates the good agreement between the experimental extraction data and the model predictions that best fit the experimental data. The averaged values of $D_{Cu^{2+}}$ and K_{Cu^{2+}/H^+}, based on three replicate extraction experiments, were determined as 6.00×10^{-15} m^2 s^{-1} and 3.65×10^{-3}, respectively. Very good agreement between the experimental data for the extraction of the CuL^+ complex from different ethanol–water solutions and the model predictions that best fitted the experimental data was also observed (Fig. 5). The self-diffusion coefficient (D_{CuL^+}) and the ion-exchange equilibrium constant (K_{CuL^+/Na^+}) in deionized water were determined as 1.87×10^{-16} m^2 s^{-1} and 109, respectively, by extrapolating the results obtained for the ethanol–water solutions mentioned above (Table 1 and Fig. 6).

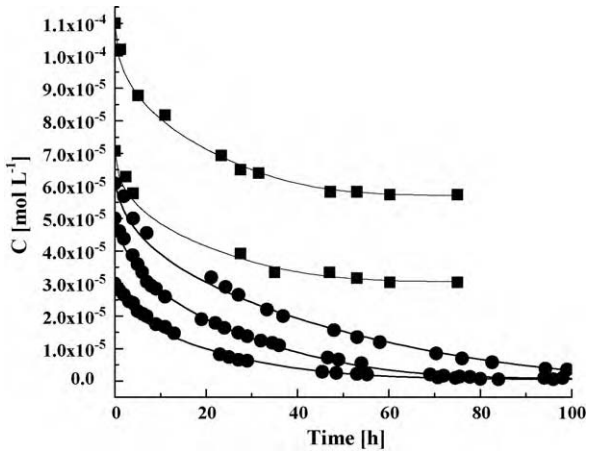

Fig. 5. Model predictions (—) that best fit the experimental extraction data for (■) Cu^{2+} (extraction from 1.10×10^{-4} and 7.08×10^{-5} mol L^{-1} aqueous solutions into Nafion membranes in their H^+ form) and (●) CuL^+ (extraction from 6.08×10^{-5} mol L^{-1} aqueous solutions containing 1.0, 3.0 or 4.0% (v/v) ethanol into Nafion membranes in their Na^+ form).

Table 1
Self-diffusion coefficient and ion-exchange equilibrium constant of CuL^+ at various ethanol concentrations.

Ethanol conc. [%, v/v]	$10^{16} \times D_{CuL^+}$ [m^2 s^{-1}]	K_{CuL^+}
0.0	1.87*	109*
1.0	2.40	150
3.0	3.80	265
4.0	5.00	380

* Extrapolated data.

4.3. Determination of the molar absorptivities of LH (ε_{LH}), LH_2^+ ($\varepsilon_{LH_2^+}$) and CuL^+ (ε_{CuL^+}) in Nafion membranes

The Nafion membranes were visibly homogenous. The molar absorptivities of the chemical species in the optode membrane (LH, LH_2^+ and CuL^+) absorbing in the visible range are presented in Table 2. The corresponding values in solutions, presented in the same table, differ considerably though the ranking order is the same. These differences could be attributed to the specific interactions between the colored species mentioned above and the membrane environment though the corresponding solution and membrane spectra were identical.

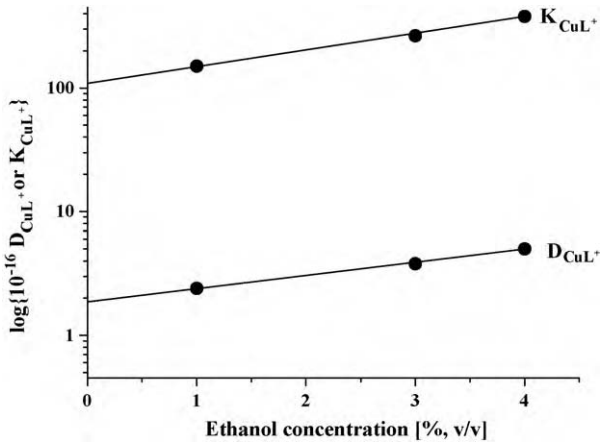

Fig. 6. $\log(K_{CuL^+})$ and $\log(10^{16} \times D_{CuL^+})$ (●) versus ethanol concentration and linear fit (—) to the data obtained for ethanol concentrations between 1.0 and 4.0% (v/v).

Table 2
Molar absorptivities at 500 nm (UV–visible spectrophotometer, 10 mm cell) of LH, LH_2^+ and CuL^+ in solution and in the Nafion membrane (optode flow-through cell).

	ε [cm L mol^{-1}]	
	Solution	Membrane
LH	7.79×10^2	3.88×10^2
LH_2^+	1.36×10^2	1.88×10^3
CuL^+	9.31×10^3	7.63×10^3

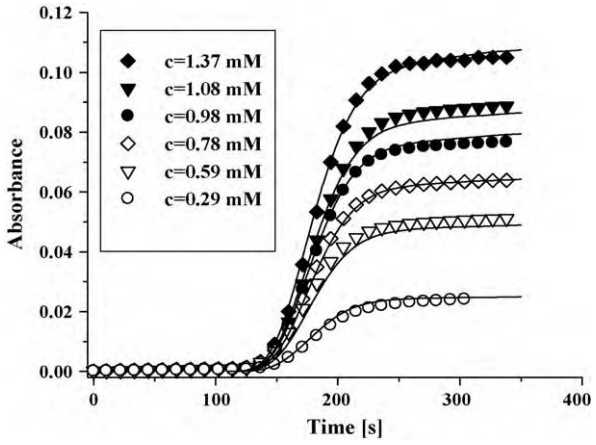

Fig. 7. Experimental and theoretically predicted (—) transient absorbance curves for six different Cu^{2+} concentrations (flow rate = 0.306 mL min^{-1}, sample volume = 14.75 μL).

4.4. Determination of the stagnant diffusion layer thickness (Δ)

As expected, there was a delay between the sensor response and the appearance of the Cu^{2+} sample zone in the optode flow-through measuring cell after the injection of a standard solution of 1.27×10^{-4} mol L^{-1} $CuSO_4$. This delay was caused by the Cu^{2+} mass-transport across the stagnant diffusion layer separating the membrane and the flowing solution (Fig. 3). The stagnant diffusion layer thickness (Δ) was varied until a satisfactory agreement between the experimental and the theoretical transient absorbance curves was obtained for $\Delta = 50$ μm. This value is of the same order of magnitude as the thickness of the stagnant diffusion layer assessed in other flow-through chemical sensors [30].

4.5. Validation of the model

Solutions of $CuSO_4$ in the concentration range from 2.90×10^{-4} to 1.37×10^{-3} mol L^{-1} were injected and the experimental transient absorbance curves obtained were compared with the corresponding theoretical model curves. All parameters used in the model simulations were those determined in the experiments outlined earlier. Very good agreement was obtained for all concentrations as illustrated in Fig. 7. As expected, similar good agreement was obtained between the experimental and the theoretical calibration curves in the concentration range studied ($A = 7.98 \times 10^{-5}$ [Cu^{2+}], where $R^2 = 0.993$).

5. Conclusions

A general mathematical model of a flow-through PAN/Nafion optode based on first principles was derived and experimentally verified in a flow injection system. All model parameters used in the experimental verification were either obtained from literature sources or determined independently as part of this study. On the basis of the results obtained it can be concluded the model outlined above can be used successfully for the mathematical description and optimization of the PAN/Nafion optode investigated as well as of other ion-exchange membrane based optodes having a similar response mechanism.

References

[1] I.L. de Mattos, M. da Cunha Areias, Talanta 66 (2005) 1281.
[2] W.H. Oldenziel, B.H.C. Westerink, Anal. Chem. 77 (2005) 5520.
[3] S. Shahrokhian, M. Ghalkhani, Electrochim. Acta 51 (2006) 2599.
[4] D.T. Newcombe, T.J. Cardwell, R.W. Cattrall, S.D. Kolev, Anal. Chim. Acta 401 (1999) 137.
[5] D.T. Newcombe, T.J. Cardwell, R.W. Cattrall, S.D. Kolev, Lab. Rob. Autom. 12 (2000) 200.
[6] L.dlC. Coo, I.S. Martinez, Talanta 64 (2004) 1317.
[7] S.C.L. Pinheiro, I.M. Raimundo Jr., Quím. Nova 28 (2005) 932.
[8] J.E. Madden, T.J. Cardwell, R.W. Cattrall, L.W. Deady, Anal. Chim. Acta 319 (1996) 129.
[9] L.dlC. Coo, T.J. Cardwell, R.W. Cattrall, S.D. Kolev, Eurosens. XII Proc. 1 (1998) 719.
[10] L.dlC. Coo, C.J. Belmonte, Talanta 58 (2002) 1063.
[11] T.J. Sands, T.J. Cardwell, R.W. Cattrall, J.R. Farrell, P.J. Iles, S.D. Kolev, Sens. Actuat. B 85 (2002) 33.
[12] B. Kuswandi, R. Narayanaswamy, Quim. Anal. (Barc.) 19 (2000) 87.
[13] M.K. Amini, T. Momeni-Isfahani, J.H. Khorasani, M. Pourhossein, Talanta 63 (2004) 713.
[14] L.dlC. Coo, T.J. Cardwell, R.W. Cattrall, S.D. Kolev, Dokl. Bulg. Akad. Nauk 54 (2001) 53.
[15] S.D. Kolev, K. Tóth, E. Lindner, E. Pungor, Anal. Chim. Acta 234 (1990) 49.
[16] K. Tóth, E. Lindner, E. Pungor, S.D. Kolev, Anal. Chim. Acta 234 (1990) 57.
[17] O. Levenspiel, K.B. Bischoff, Adv. Chem. Eng. 4 (1963) 95.
[18] S.D. Kolev, E. Pungor, Talanta 34 (1987) 1009.
[19] S.D. Kolev, Anal. Chim. Acta 308 (1995) 36.
[20] G. Taylor, Proc. R. Soc. Lond. A 219 (1953) 186.
[21] G. Taylor, Proc. R. Soc. Lond. A 225 (1954) 473.
[22] D.T. Newcombe, T.J. Cardwell, R.W. Cattrall, S.D. Kolev, J. Membr. Sci. 141 (1998) 155.
[23] L.dlC. Coo, T.J. Cardwell, R.W. Cattrall, S.D. Kolev, Anal. Chim. Acta 392 (1999) 201.
[24] Z. Samec, A. Trojánek, E. Samcová, J. Phys. Chem. 98 (1994) 6352.
[25] S.D. Kolev, Sep. Sci. Technol. 38 (2003) 237.
[26] G.A. Korn, T.M. Korn, Mathematical Handbook for Scientists and Engineers, fourth ed., McGraw-Hill, New York, 1968.
[27] R.W. Hamming, Numerical Methods for Scientists and Engineers, McGraw-Hill, New York, 1962.
[28] B. Carnahan, H.A. Luther, J.O. Wilkes, Applied Numerical Methods, J. Wiley, New York, 1969.
[29] L.dlC. Coo, T.J. Cardwell, R.W. Cattrall, S.D. Kolev, Anal. Chim. Acta 360 (1998) 153.
[30] S.D. Kolev, C.W.K. Chow, D.E. Davey, D.E. Mulcahy, Anal. Chim. Acta 329 (1996) 1.
[31] S.D. Kolev, E. Pungor, Anal. Chem. 60 (1988) 1700.